(arrow head) and diffuse plaques (arrow) of AD brains, respectively (400X). (I-K) Determinations of number of intraneuronal AβO immunolabelling in human brains: 1A9 (panel I), 2C3 (panel J), and A11 (panel K). Designations used herein were as follows: Granular, dense granule staining; Diffuse, diffuse staining; None, no staining; NC, normal control; AD, Alzheimer's disease. Experimental results of staining pattern were analyzed by one-way ANOVA, followed by Dannett's test for posthoc analysis: statistical significance compared with NC (*p<0.01, **p<0.001).

Figure 4. Cell uptake of neurotoxic AβOs. (A) SH-SY5Y cells were exposed to Fluor™ 488 alone, 5 μM HiLyte Fluor™ 488-labeled AβMs or AβOs (green) at 37℃ for 10, 30, and 180 min. AβMs: 10 kDa-filtrate; AβOs:30 kDa-retentate. Nuclear staining (7-AAD) is shown in red. Vesicular uptake was observed with AβOs, but not with AβMs and Fluor™ 488 alone. (B) The level of LDH released from SH-SY5Y cells treated for the indicated times (0, 3, 6, and 24 h) with 5 μM AβOs. In the case of 5 μM synthetic Aβ42-1 and AβMs, LDH assay was done for 24 h. Each value indicates the percentage level of LDH released following treatment with incubation mixtures relative to the level of LDH released following treatment with Triton X-100. Each column indicates average ± S.D. The p value was determined by one-way

ANOVA, followed by Dannett's test for posthoc analysis: statistical significance compared with AβMs alone (*p<0.05, **p<0.001).

Figure 5. Passive immunization protects Tg2576 mice from memory deficits. Tg2576 mice at 13 months of age in three groups were studied: PBS-treated non-Tg mice, n=14; PBS-treated Tg2576 mice, n=10; 1A9-treated mice, n=13; 2C3-treated mice, n=12. Values indicate the mean ± SEM . (A) Y-maze test. Spontaneous alternation behavior during an 8-min session in the Y-maze task was measured in each group. Results of one-way ANOVA were as follows: F(3, 45)= 2.99, p<0.05, **p<0.05 vs PBS-treated non-Tg mice, #p<0.05 vs PBS-treated Tg2576 mice. (B) Novel object recognition test. The retention session was carried out 24 h after the training. Exploratory preference during a 10-min session in the novel-object recognition test was measured in each group. Results of the two-way ANOVA were as follows: training/retention, F(1, 90)=58.19, p<0.01; animal group, F(3, 90)=6.18, p<0.01; interation of training/retention with animal group, F(3, 90)=7.57, p<0.01; **p<0.01 vs corresponding trained mice. ##p<0.01 vs PBS-treated non-Tg mice, ††p<0.01 vs PBS-treated Tg2576 mice. (C) Swimming-path length during a 60-s session in the water maze test was measured in each group. Results of the two-way ANOVA were as

follows: trial, F(9, 450)=25.51, p<0.01; animal group, F(3, 450)=14.85, p<0.01; interaction of trial with animal group, F(27, 450)= 1.36, p=0.11; **p<0.01 vs PBS-treated non-Tg mice, #p<0.05, ##p<0.01 vs PBS-treated Tg2576 mice. Conditioned fear learning test: context-dependent (D) and cue-dependent (E) freezing times were measured. The results of one-way ANOVA were as follows: context-dependent test, F(3, 45)= 6.19, p<0.01; cue-dependent test, F(3, 45)=5.41, *p<0.05; **p<0.01 vs PBS-treated non-Tg mice, #p<0.05, ##p<0.01 vs PBS-treated Tg2576 mice.

Figure 6. Passive immunization protects Tg2576 mice from synaptic or neuronal degeneration. (**A**) Saline-insoluble, SDS-extractable synaptic proteins were examined by Western blot analysis and probed for PSD95 (1:250), drebrin (DB, 1:100), and synaptophysin (SYP, 1:2000). The p value was determined by one-way ANOVA: *p<0.05. Representive Confocal immunofluorescence microscopy images of Tg2576 mouse brain. Sections of the cortex of the untreated (PBS)-, 1A9-treated, or 2C3-treatedTg2576 mouse brain were immunostained with PSD-95 (Upper part of panel A), Derbrin (DB, Middle part of panel A), synaptophysin (SYP, Lower part of panel A). Scale bar = 30 μm. (**B**) Confocal immunofluorescence microscopy images

of Tg2576 mouse brain. Sections of the hippocampus of the untreated (PBS)-, 1A9-treated, or 2C3-treatedTg2576 mouse brain were immunostained with Fluoro Jade B (1:50000). Scale bar = 100 μm. (**C**) Representive Confocal immunofluorescence microscopy images of AD brain. Sections of the hippocampus of AD brains were immunostained with Fluoro Jade B. Scale bar = 20 μm.

Figure 7. Passive immunization protects Tg2576 mice from accumulation of intraneuronal AβOs. Dot blot immunoassay for A11-immunoreactive AβOs in saline-soluble extracts (**A**), saline-insoluble, SDS-extractable extracts (**B**), and SDS-insoluble, FA-extractable extracts (**C**) obtained from untreated, 1A9-treated, or 2C3-treated mice (30 μg of total extracted brain protein per dot). Results from densitometric imaging of these same samples. The line indicates the mean of each set. The *p* value was determined by one-way ANOVA: $*p<0.05$, $**p<0.001$. (**C**) Confocal immunofluorescence microscopy images of Tg2576 mouse brain. Sections of the hippocampus of the Tg2576 mouse brain were doubly immunostained with 7-AAD (red, 1:50) and anti-A11 antibody (green, 1:250). Scale bar = 10 μm.

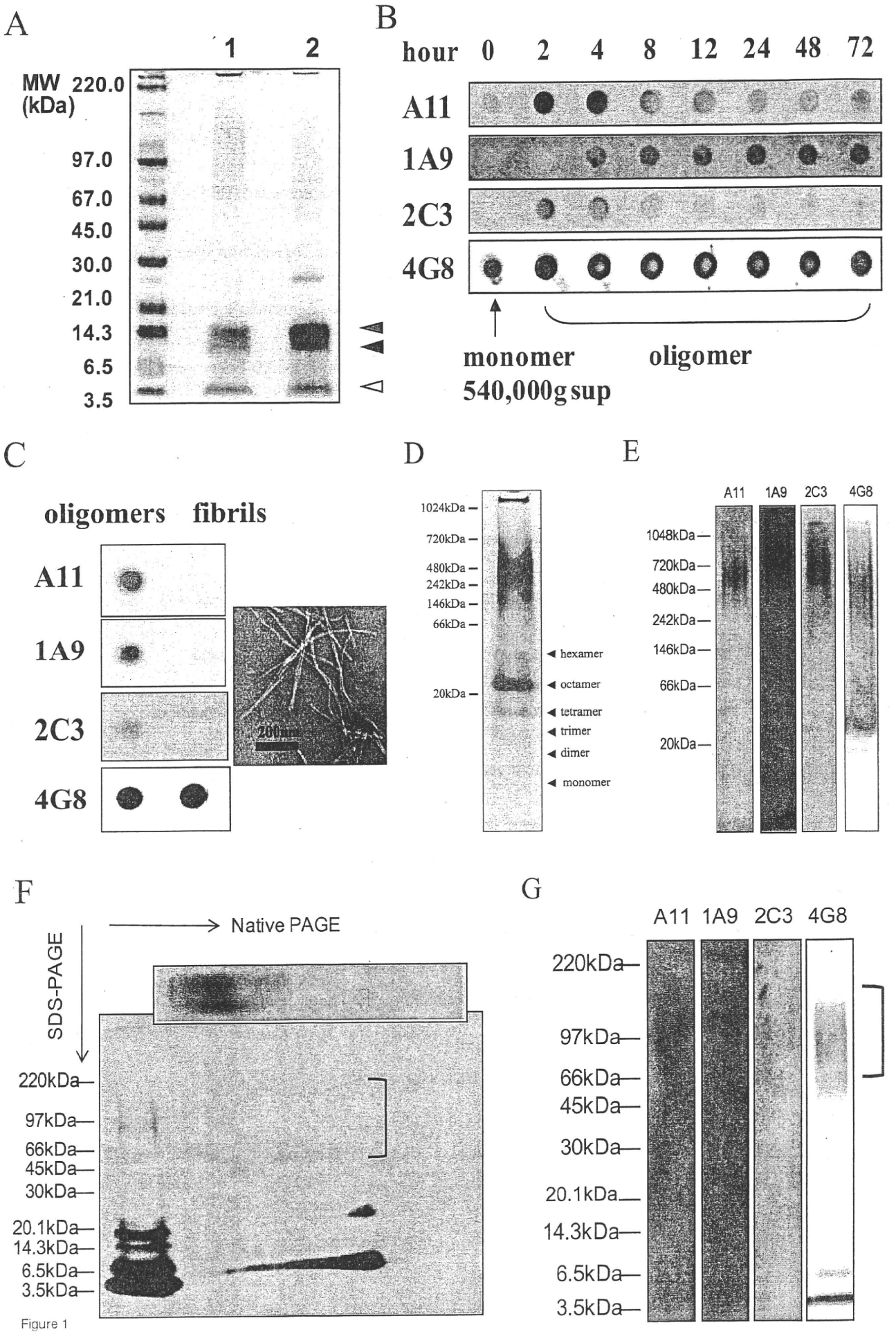
A
1
2
MW (kDa)
220.0
97.0
67.0
45.0
30.0
21.0
14.3
6.5
3.5
B
hour 0 2 4 8 12 24 48 72
A11
1A9
2C3
4G8
monomer
oligomer
540,000g sup
C
oligomers fibrils
A11
1A9
2C3
4G8
200nm
D
1024kDa
720kDa
480kDa
242kDa
146kDa
66kDa
20kDa
hexamer
octamer
tetramer
trimer
dimer
monomer
E
A11 1A9 2C3 4G8
1048kDa
720kDa
480kDa
242kDa
146kDa
66kDa
20kDa
F
Native PAGE
SDS-PAGE
220kDa
97kDa
66kDa
45kDa
30kDa
20.1kDa
14.3kDa
6.5kDa
3.5kDa
G
A11 1A9 2C3 4G8
220kDa
97kDa
66kDa
45kDa
30kDa
20.1kDa
14.3kDa
6.5kDa
3.5kDa

Figure 1

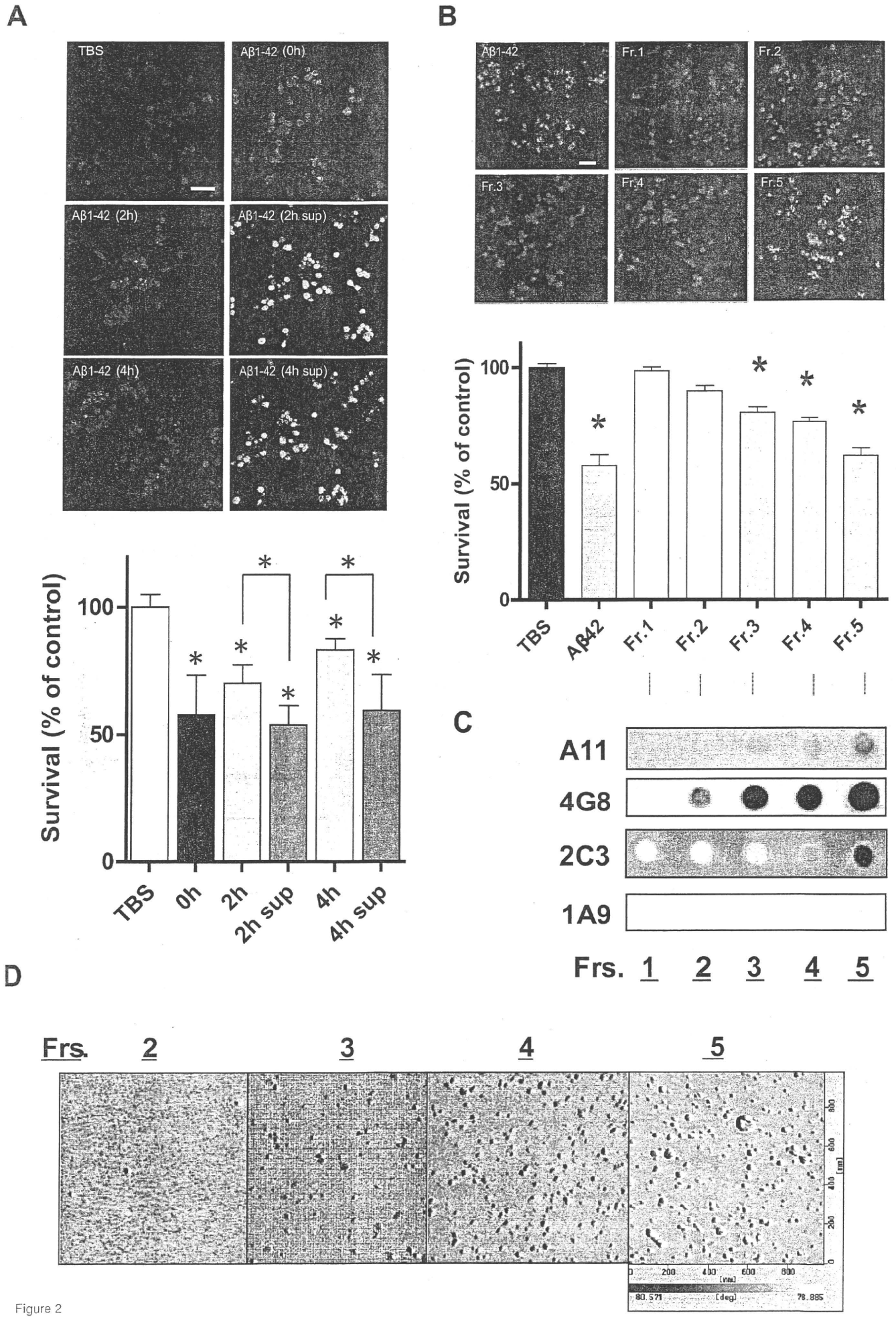
A
TBS
Aβ1-42 (0h)
Aβ1-42 (2h)
Aβ1-42 (2h sup)
Aβ1-42 (4h)
Aβ1-42 (4h sup)
Survival (% of control)
100
50
0
TBS
0h
2h
2h sup
4h
4h sup
B
Aβ1-42
Fr.1
Fr.2
Fr.3
Fr.4
Fr.5
Survival (% of control)
100
50
0
TBS
Aβ42
Fr.1
Fr.2
Fr.3
Fr.4
Fr.5
C
A11
4G8
2C3
1A9
Frs. 1 2 3 4 5
D
Frs. 2 3 4 5

Figure 2

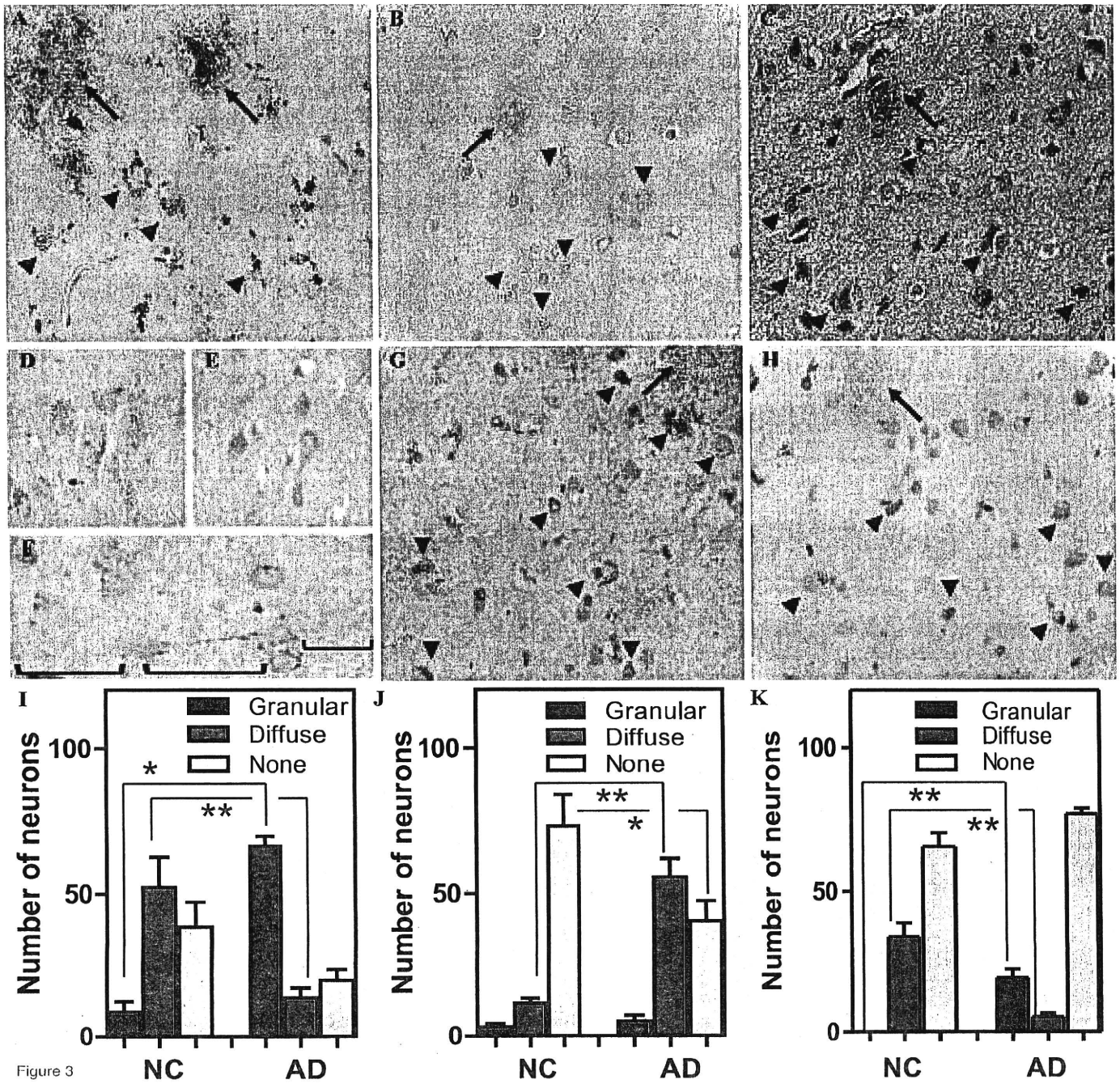
A
B
C
D
E
F
G
H
I
J
K
Granular
Diffuse
None
Number of neurons
100
50
0
*
**
NC
AD

Figure 3

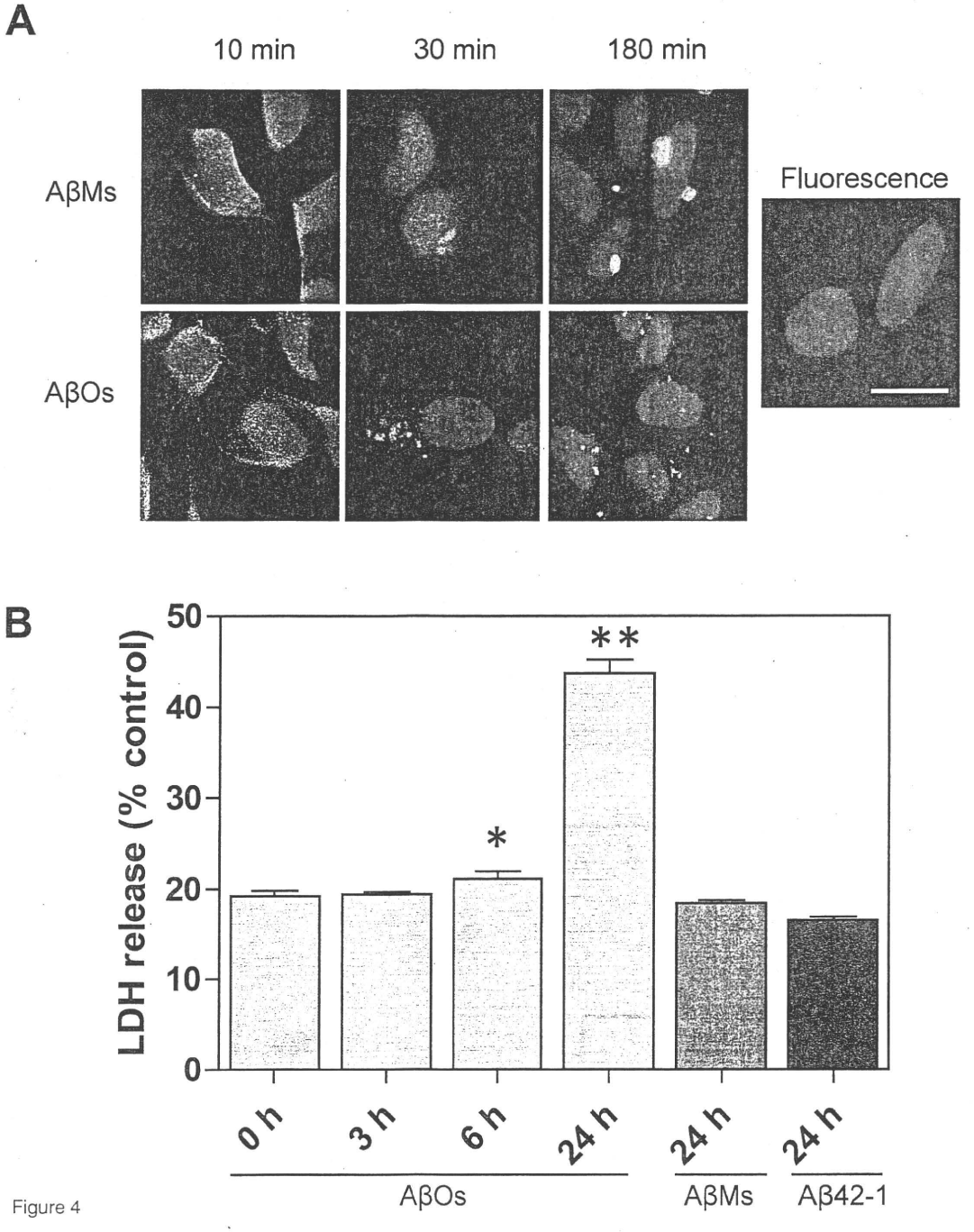
A
10 min
30 min
180 min
AβMs
AβOs
Fluorescence
B
LDH release (% control)
50
40
30
20
10
0
**
*
0 h
3 h
6 h
24 h
24 h
24 h
AβOs
AβMs
Aβ42-1

Figure 4

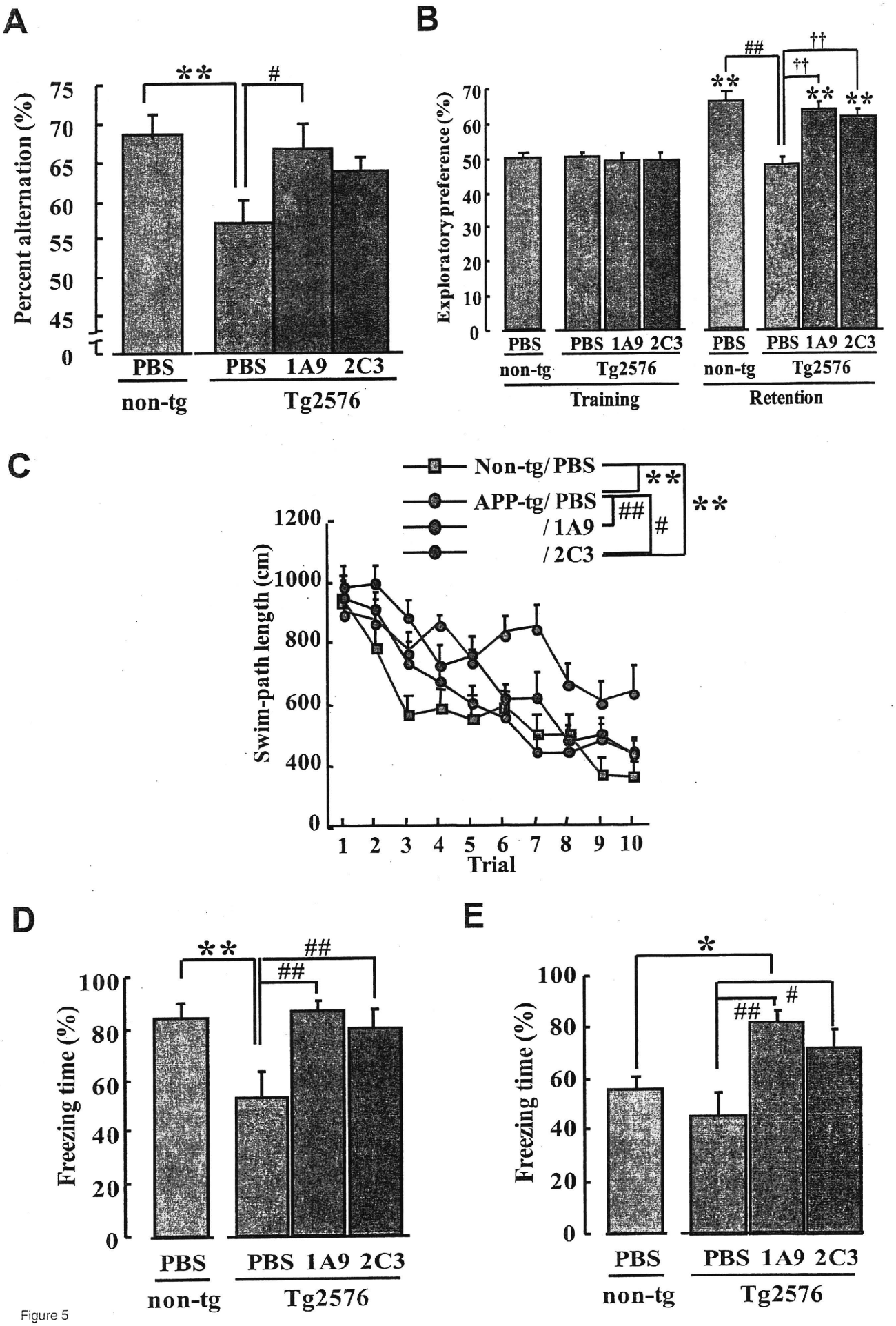
A
Percent alternation (%)
75
70
65
60
55
50
45
0
**
#
PBS
PBS 1A9 2C3
non-tg
Tg2576
B
Exploratory preference (%)
70
60
50
40
30
20
10
0
##
††
††
**
**
**
PBS
PBS 1A9 2C3
PBS
PBS 1A9 2C3
non-tg
Tg2576
non-tg
Tg2576
Training
Retention
C
Non-tg/ PBS
APP-tg/ PBS
/ 1A9
/ 2C3
**
##
#
**
Swim-path length (cm)
1200
1000
800
600
400
0
1 2 3 4 5 6 7 8 9 10
Trial
D
Freezing time (%)
100
80
60
40
20
0
**
##
##
PBS
PBS 1A9 2C3
non-tg
Tg2576
E
Freezing time (%)
100
80
60
40
20
0
*
#
##
PBS
PBS 1A9 2C3
non-tg
Tg2576

Figure 5

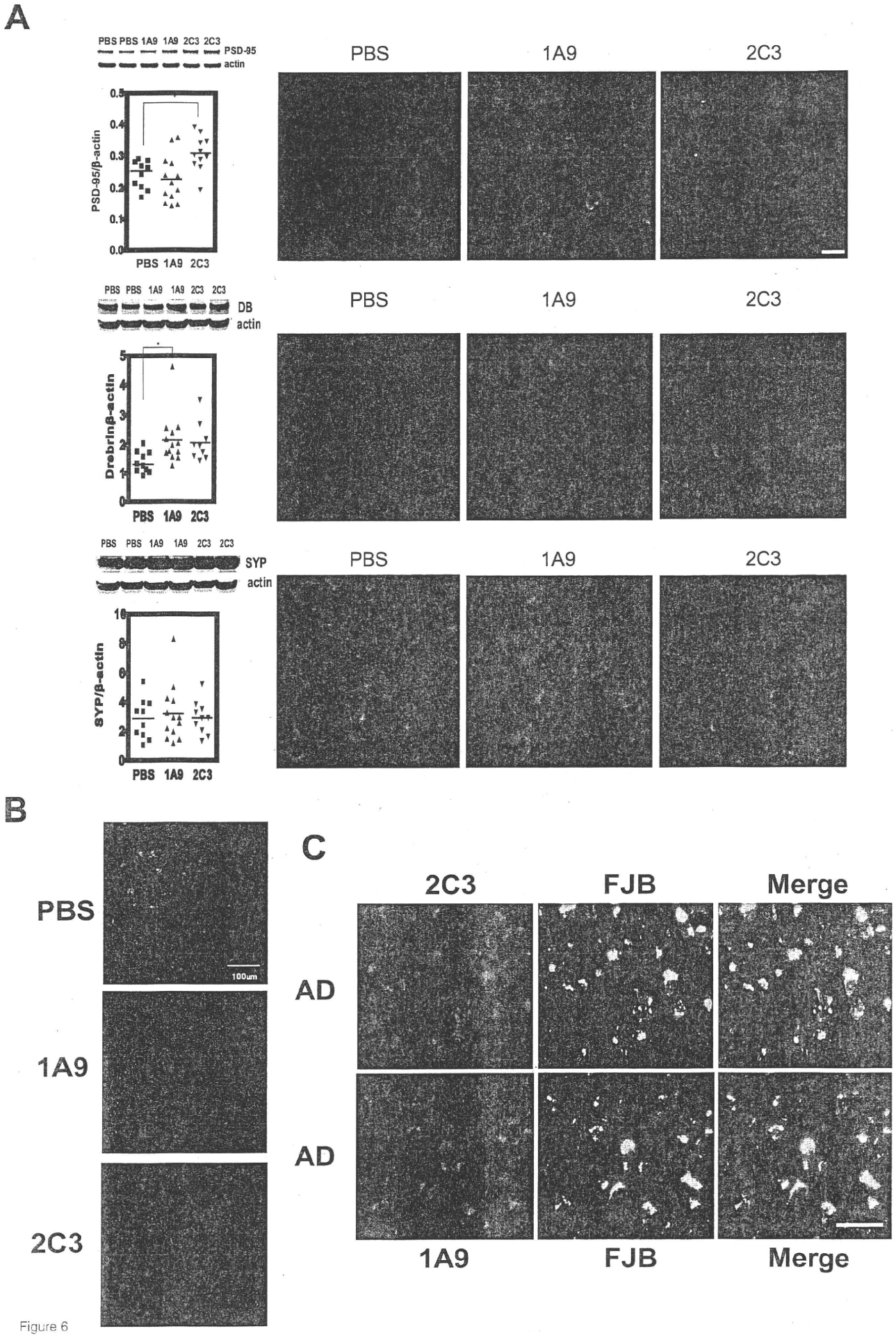
A
PBS PBS 1A9 1A9 2C3 2C3
PSD-95
actin
PSD-95/β-actin
PBS 1A9 2C3
PBS
1A9
2C3
DB
Drebrin/β-actin
SYP
SYP/β-actin
B
PBS
1A9
2C3
100um
C
2C3
FJB
Merge
AD
AD
1A9
FJB
Merge

Figure 6

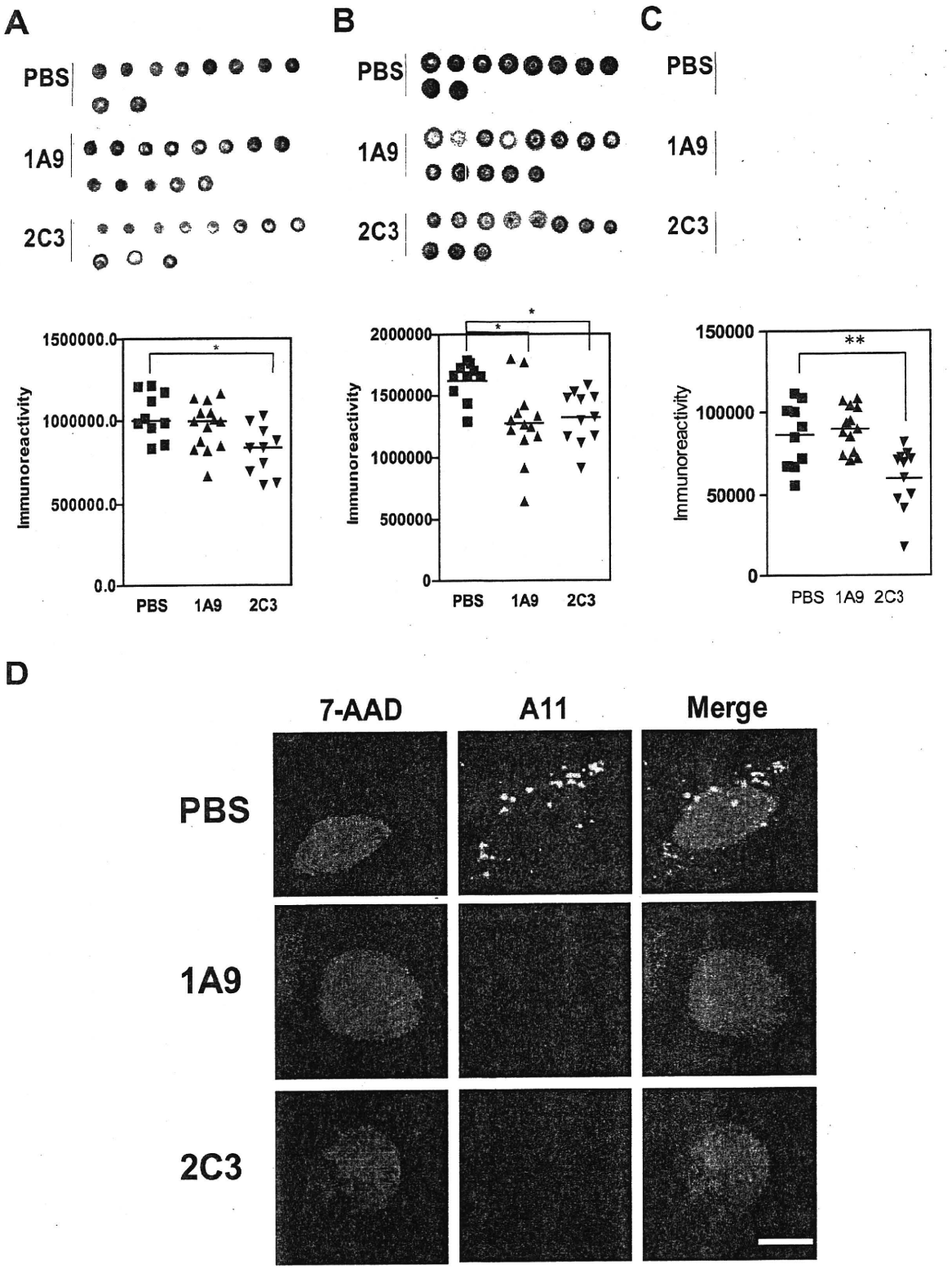
A
PBS
1A9
2C3
B
PBS
1A9
2C3
C
PBS
1A9
2C3
Immunoreactivity
1500000.0
1000000.0
500000.0
0.0
PBS 1A9 2C3
Immunoreactivity
2000000
1500000
1000000
500000
0
PBS 1A9 2C3
Immunoreactivity
150000
100000
50000
0
PBS 1A9 2C3
D
7-AAD
A11
Merge
PBS
1A9
2C3

Figure 7

Biochemical and Biophysical Research Communications 402 (2010) 54–58

Contents lists available at ScienceDirect

Biochemical and Biophysical Research Communications

journal homepage: www.elsevier.com/locate/ybbrc

Potent inhibitors of amyloid β fibrillization, 4,5-dianilinophthalimide and staurosporine aglycone, enhance degradation of preformed aggregates of mutant Notch3

Keikichi Takahashi, Kayo Adachi [1], Shohko Kunimoto [1], Hideaki Wakita [1], Kazuya Takeda *[,1], Atsushi Watanabe *[,1]

Department of Vascular Dementia Research, National Institute for Longevity Sciences, National Center for Geriatrics and Gerontology (NCGG), Aichi, Japan

ARTICLE INFO

Article history:
Received 14 September 2010
Available online 1 October 2010

Keywords:
CADASIL
Vascular dementia
Notch3
Protein aggregation
Low-molecular compound

ABSTRACT

Cerebral autosomal dominant arteriopathy with subcortical infarcts and leukoencephalopathy (CADASIL) is caused by mutations in human *NOTCH3*. We have recently reported that mutant Notch3 shows a greater propensity to form aggregates, and these aggregates resist degradation, leading to accumulation in the endoplasmic reticulum (ER). In this study, we searched for low-molecular compounds that decrease the amount of mutant Notch3 aggregates. Using a cell-based system, we found that degradation of preformed mutant aggregates was enhanced by treatment with either 4,5-dianilinophthalimide (DAPH) or staurosporine aglycone (SA), both of which inhibit amyloid β (Aβ) fibrillization. Regarding other low-molecular compounds interacting with Aβ fibrils, thioflavin T (ThT) also enhanced the clearance of mutant Notch3. These findings suggest that DAPH, SA, and ThT are potent reagents to dissociate the preformed aggregates of mutant Notch3 by disruption of intermolecular contacts of misfolded proteins. Our study may provide the basis for the development of a pharmacological therapy for CADASIL.

1. Introduction

Cerebral autosomal dominant arteriopathy with subcortical infarcts and leukoencephalopathy (CADASIL) is a hereditary small vessel disease causing recurrent subcortical ischemic strokes and vascular dementia [1–3]. The pathological hallmarks of the disorder are degeneration of vascular smooth muscle cells (VSMCs) and the abnormal accumulation of granular osmiophilic material (GOM) [4,5]. CADASIL is caused by missense mutations and small deletions in *NOTCH3* [6,7], and the extracellular domain of Notch3 is a constituent of GOM [8]. Although the formation of GOM is considered to be involved in the disease process, the molecular mechanisms by which Notch3 mutations lead to vascular degeneration remain unclear [9–16]. Recently, we have shown that mutant Notch3 is more prone to form aggregates that are accumulated in the endoplasmic reticulum (ER) and is considerably resistant to ER-associated degradation (ERAD) than wild-type Notch3 [17]. These findings indicate that the cytotoxic effects of mutant Notch3 may be related to the formation and accumulation of mutant aggregates in the ER.

In the present study, we searched for low-molecular compounds that efficiently degrade the preformed aggregates of mutant Notch3. Using tetracycline (Tet)-on inducible stable cell lines, we found that the degradation of preformed mutant aggregates was facilitated by treatment with 4,5-dianilinophthalimide (DAPH) and staurosporine aglycone (SA), which inhibit amyloid β (Aβ) fibrillization [18,19]. Furthermore, thioflavin T (ThT), which interacts with Aβ fibrils and senile plaques [20], also accelerated the clearance of mutant Notch3 aggregates. These findings may invigorate hope for a pharmacological therapy of CADASIL patients.

2. Materials and methods

2.1. Low-molecular compounds

4,5-Dianilinophthalimide (DAPH), staurosporine aglycone (SA), and trehalose were purchased from Sigma. Tauroursodeoxycholic

Abbreviations: CADASIL, cerebral autosomal dominant arteriopathy with subcortical infarcts and leukoencephalopathy; ER, endoplasmic reticulum; DAPH, 4,5-dianilinophthalimide; SA, staurosporine aglycone; Aβ, amyloid β; ThT, thioflavin T; VSMCs, vascular smooth muscle cells; GOM, granular osmiophilic material; ERAD, ER-associated degradation; Tet, tetracycline; TUDCA, tauroursodeoxycholic acid; 4PBA, 4-phenylbutyric acid; ThS, thioflavin S; PIB, Pittsburgh compound-B; HEK, human embryonic kidney.

* Corresponding authors. Address: Department of Cognitive Brain Science, Research Institute, National Center for Geriatrics and Gerontology (NCGG), 35 Gengo, Morioka, Obu, Aichi 474-8511, Japan. Fax: +81 562 46 8438.

E-mail addresses: ktakeda@ncgg.go.jp (K. Takeda), watsushi@ncgg.go.jp (A. Watanabe).

[1] Present address: Department of Cognitive Brain Science, Research Institute, National Center for Geriatrics and Gerontology (NCGG), Aichi, Japan.

0006-291X/$ - see front matter © 2010 Elsevier Inc. All rights reserved.
doi:10.1016/j.bbrc.2010.09.105

acid (TUDCA) was from Calbiochem, and thioflavin T (ThT), curcumin, and 4-phenylbutyric acid (4PBA) were from Wako. Thioflavin S (ThS) was from ICN Biomedicals. Tetrahydrocurcumin and resveratrol were kind gifts from Dr. Wakako Maruyama (National Center for Geriatrics and Gerontology). Pittsburgh compound-B (PIB), that is, 2-(4′-methylaminophenyl)-6-hydroxybenzothiazole [21], was a gift from Dr. Seiji Iwasa (Toyohashi University of Technology).

2.2. Stable cell lines

We previously established stable human embryonic kidney (HEK) 293 cell lines in which the expression of Notch3 can be induced using the Tet-on regulatory system (T-Rex system; Invitrogen) [17]. Several cell lines expressing either wild-type or mutant [arginine 133 to cysteine (p.R133C) or cysteine 185 to arginine (p.C185R)] human Notch3 were obtained [17]. The stable cell lines were maintained in DMEM containing 10% fetal bovine serum, 200 μg/ml Zeocin (Invitrogen), and 10 μg/ml blasticidin-S (Invitrogen).

2.3. Western blot analysis

Cells (1.2×10^6) were seeded in six-well plates, treated with 2 μg/ml tetracycline for 24 h, and then cultured in a fresh medium without tetracycline. For treatment of low-molecular compounds, the cells were incubated in the medium containing one of these compounds for 2 days. At indicated times, the cells were harvested and lysed in solution A containing 1% Triton X-100, 0.1 M Tris–HCl (pH 7.4), 0.15 M NaCl, and a protease inhibitor cocktail (Boehringer Mannheim). Lysates (30 μg/lane) were separated on a 7–10% SDS–polyacrylamide gel, and the separated proteins were transferred to a nitrocellulose membrane (Bio-Rad). The membrane was blocked in TBST [10 mM Tris–HCl (pH 7.4), 150 mM NaCl, 0.1% Tween-20] containing 5% nonfat milk and probed using the following the primary and secondary antibodies: a rabbit polyclonal anti-human Notch3 antibody (AbN2, 1 μg/ml) [14,17] and a mouse monoclonal anti-GAPDH antibody (Sigma, 1:2000); a HRP-conjugated goat anti-rabbit antibody (BD Biosciences, 1:3000) and a HRP-conjugated sheep anti-mouse antibody (GE Healthcare, 1:2000). Immunoreactive proteins were detected using Western Lightning chemiluminescence reagents (Perkin Elmer). Protein concentration was determined by micro-BCA assay (Pierce).

2.4. Immunocytochemistry

Cells were cultured in 35-mm Petri dishes coated with poly-L-lysine and fixed in 4% paraformaldehyde in PBS at 4 °C for 10 min. After treatment with 0.2% Triton X-100 for 10 min, cells were blocked with PBS containing 3% fetal bovine serum for 30 min and incubated for 1 h with an anti-Notch3 antibody (AbN2, 1 μg/ml) at room temperature. Cells were washed three times with PBS and incubated for 1 h with a Rhodamine Red-labeled goat anti-rabbit antibody (Molecular Probes) at a 1:1000 dilution in PBS. After three washes in PBS, cells were examined under a light microscope (Olympus). Cells with aggregates were quantified manually by counting cell numbers in phase contrast and immunofluorescence microscopy images and scored as the percentage of the total number of cells.

2.5. Statistical analysis

Data are presented as means ± standard deviation (S.D.). Statistical analysis was performed using unpaired *t*-test (two-tailed) or one-way ANOVA with Dunnett's multiple comparison post hoc test (PRISM version 5.0a; GraphPad Software, La Jolla, CA, USA). Values of $P < 0.05$ were considered significant.

3. Results

3.1. Effects of low-molecular compounds on clearance of mutant Notch3

We established stable HEK293 cell lines in which expression of Notch3 was inducible using the Tet-on regulatory system and showed by pulse-chase analysis and Western blot analysis that the aggregates of mutant Notch3 resisted degradation and accumulated in the ER [17]. Because the expression of Notch3 could be induced and silenced by adding and removing tetracycline, respectively, the degradation rate of Notch3 is easily determined by Western blot analysis. As shown in Fig. 1A, wild-type Notch3 rapidly disappeared within 1 day after silencing its expression, whereas considerable amounts of mutant Notch3 were still detected after 2 days.

Using these cell lines, we searched for low-molecular compounds that facilitated the degradation of the mutant Notch3 aggregates. Previous studies have shown that the chemical

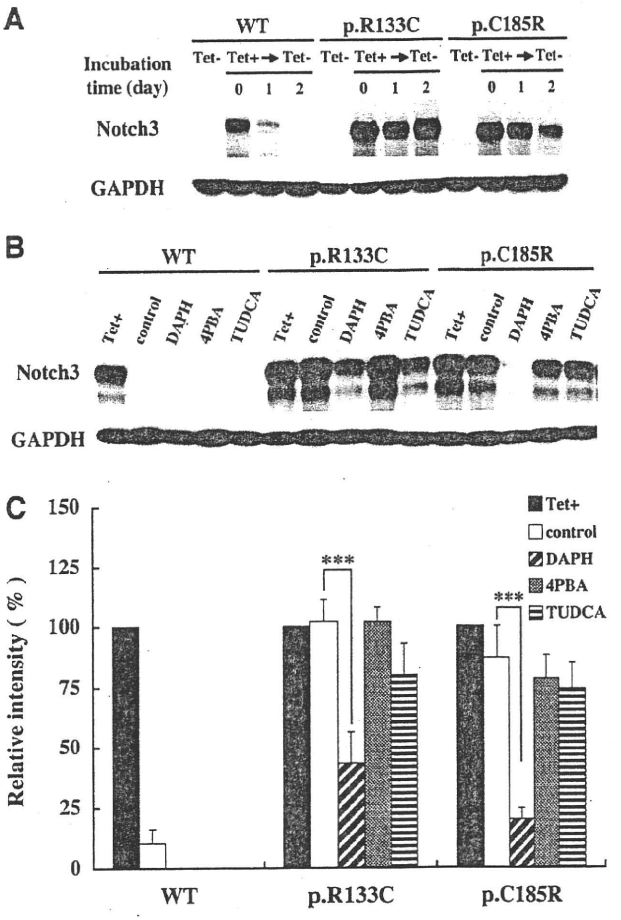

Fig. 1. Effects of low-molecular compounds on degradation of mutant Notch3. (A) Cells were treated with (Tet+) and without (Tet−) 2 μg/ml tetracycline for 24 h and then incubated in the standard medium. The cells were harvested at the indicated times (0–2 days) after the medium change and subjected to Western blot analysis. A representative Western blot is shown. (B) After treatment with 2 μg/ml tetracycline for 24 h (Tet+), cells were incubated in the standard medium with 10 μM DAPH, 20 mM 4PBA or 20 mM TUDCA and without a chemical compound (control) for 2 days. A representative Western blot is shown. (C) Densitometry of the Western blot (B) were performed to estimate relative amounts of wild-type Notch3 and mutant Notch3. Results represent means ± S.D. of data from five experiments and are shown as the percentage of Tet+. ***, $P < 0.001$ relative to untreated cells (control) for each cell line.

chaperones 4PBA and TUDCA modulate the stability of the mutant proteins and inhibit the formation of aggregates [22–24]. In addition, DAPH has been reported to inhibit and reverse the formation of Aβ42 fibrils [18,19]. Therefore, we investigated the effects of these compounds on the clearance of mutant Notch3 aggregates. Stable cells were treated with these compounds for 2 days after stopping the expression of Notch3. As shown in Fig. 1B, treatment with DAPH markedly decreased the amount of mutant Notch3, indicating that this compound effectively enhanced the degradation of mutant Notch3. The amount of mutant Notch3 slightly decreased in cells treated with either 4PBA or TUDCA, although the effect varied among different cell lines expressing mutant Notch3. Quantitative analysis of data showed that only treatment with DAPH resulted in a significant decrease in the amount of mutant Notch3 (Fig. 1C).

3.2. DAPH enhances degradation of mutant Notch3

We determined the effect of DAPH on the clearance of the mutant Notch3 aggregates by immunocytochemical analysis of stable cells using an anti-Notch3 antibody (AbN2). As shown in Fig. 2A, treatment with DAPH significantly decreased the number of cells containing mutant aggregates. Quantitative immunocytochemical analysis revealed that the percentage of cells with mutant Notch3 aggregates to total cells decreased from 35% to 18% for cells expressing the p.R133C mutant and from 33% to 9% for cells expressing the p.C185R mutant following DAPH treatment (Fig. 2B). These results indicate that DAPH enhances the degradation of preformed aggregates of mutant Notch3.

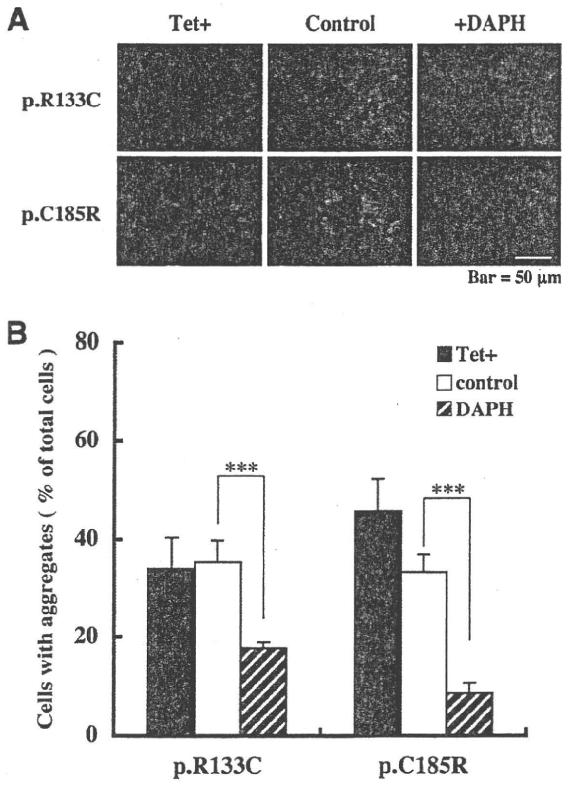

Fig. 2. Effect of DAPH on degradation of preformed mutant aggregates. Cells were treated with 2 μg/ml tetracycline for 24 h (Tet+) and then incubated in the standard medium with 10 μM DAPH or without DAPH (control) for 2 days. (A) Cells were fixed and stained with an anti-Notch3 antibody. Representative photographs are shown. Scale bar, 50 μm. (B) Cells with aggregates were quantified manually by counting cell number 0 day (Tet+) and 2 days after treatment of DAPH. Results represent means ± S.D. of data from five independent images and are shown as the percentage of total number of cells. ***$P < 0.001$ relative to untreated cells (control) of each cell line.

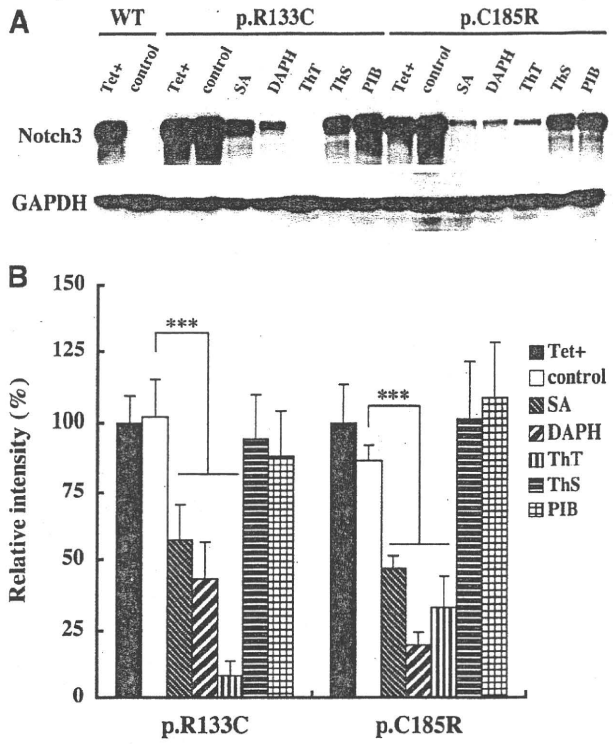

Fig. 3. Effects of Aβ-binding compounds on degradation of mutant Notch3. (A) Cells were treated with 2 μg/ml tetracycline for 24 h (Tet+) and then incubated in the standard medium with 20 μM SA, 10 μM DAPH, 2 μM ThT, 40 μM ThS, or 40 μM PIB and without a chemical compound (control) for 2 days. Cells were lysed and subjected to Western blot analysis. A representative Western blot is shown. (B) Densitometry of the Western blot was performed to estimate relative amounts of mutant Notch3. Results represent means ± S.D. (DAPH $n = 6$, others $n = 4$) and are shown as the percentage of Tet+. ***$P < 0.001$ relative to untreated cells (control) for each cell line.

3.3. Identification of other low-molecular compounds as enhancers of mutant Notch3 degradation

Because DAPH has been reported to inhibit Aβ42 fibrillization [18,19], we determined the effects of other compounds that interact with either Aβ fibrils or amyloid deposits (Fig. 3A and B). SA, an analog of DAPH, was less effective in degrading mutant Notch3 aggregates than DAPH. ThT and ThS, both of which bind the β-sheet structure of amyloid deposits [20], showed their contrasting effects on the degradation of mutant Notch3, the former was more potent than DAPH for the p.R133C mutant, but the latter did not decrease the amount of mutant Notch3. PIB, an amyloid-imaging probe of PET [21], did not degrade mutant Notch3. As shown in Table 1, we also analyzed several compounds including antioxidants (tetrahydrocurcumin and resveratrol), an autophagy inducer (trehalose) [25] and an inhibitor of Aβ aggregation (curcumin) [26]. However, these compounds did not decrease the amount of mutant Notch3, suggesting that the degradation of mutant Notch3 was facilitated by a limited type of inhibitor of Aβ fibrillization.

4. Discussion

Using stable HEK293 cell lines with inducible expression of mutant Notch3, we have shown that the degradation of preformed

Table 1
Summary of effects of low-molecular compounds on degradation of Notch3 aggregates.

Compound	Conc.	Effect	Function
4,5-Dianilinophthalimide (DAPH)	(10 μM)	+++	Inhibitor of Aβ fibrillization
Staurosporine aglycone (SA)	(20 μM)	++	DAPH analog and apoptosis inducer
Thioflavin T (ThT)	(2 μM)	+++	Bind to Aβ and senile plaques
Thioflavin S (ThS)	(40 μM)	–	Bind to Aβ and senile plaques
Curcumin	(30 μM)	–	Inhibitor of Aβ aggregation
PIB	(40 μM)	–	Imaging probe for senile plaques
4-Phenylbutyric acid (4PBA)	(20 mM)	–	Chemical chaperone
Tauroursodeoxycholic acid (TUDCA)	(20 mM)	–	Chemical chaperone
Trehalose	(20 mM)	–	Autophagy inducer
Tetrahydrocurcumin	(20 μM)	–	Antioxidant
Resveratrol	(20 μM)	–	Antioxidant

The effects of chemical compounds were determined as described in Fig. 1C and Fig. 3B. Triple plus (+++) and double plus (++) signs indicate the strong and mild elimination effects on mutant aggregates, respectively. Minus (–) signs represent the insignificant degradation effect on mutant aggregates.

mutant Notch3 aggregates is enhanced by treatment with low-molecular compounds, namely, DAPH and SA, which are novel reagents preventing fibril formation and the neurotoxicity of Aβ42 peptides [18,19]. However, the exact mechanisms of clearing mutant Notch3 aggregates by the inhibitors of Aβ fibrillization are unclear. Previous study using a cell-free system had indicated that DAPH and its analogs change the β-sheet conformation of amyloid fibrils by inhibiting and disrupting the formation of intermolecular contacts, although SA was less potent in inhibiting Aβ fibrillization than DAPH [19]. Because DAPH shows no effect on fiber assembly or disassembly of Tau, α-synuclein and Ure2 [19], the compounds may interact with a specific conformational element of Aβ42 fibrils. Thus, it is likely that DAPH might also recognize a common structure in mutant Notch3 aggregates and disrupt intermolecular contacts of mutant Notch3, resulting in the dissociation and degradation of the aggregates. In addition, ThT showed the ability to degrade aggregates of mutant Notch3. Interestingly, the clearance of mutant Notch3 aggregates was enhanced by the treatment with ThT but not ThS, although both compounds have been known to interact with β-sheet-containing Aβ fibrils and are used as a fluorescence probe to analyze β-sheet formation [20]. Thus, ThT but not ThS may interact with the common element in mutant aggregates that is recognized by DAPH. On the other hand, our previous study has indicated that mutant Notch3 is more prone to form aggregates compared with wild-type Notch3, and mutant aggregates impairs cell proliferation [17]. Therefore, we examined whether DAPH could promote cell proliferation. However, DAPH mildly attenuates cell growth. For this reason, we could not evaluate the exact effect of DAPH on cell proliferation by enhancing the degradation of mutant aggregates in the present study.

Several low-molecular compounds have also been reported to reverse the misfolding of mutant membrane and secretory proteins. 4PBA and TUDCA are chemical chaperones that stabilize protein conformation, improve ER folding capacity, and facilitate the trafficking of mutant proteins [23,24,27]. Trehalose is an autophagy enhancer and inhibits the formation of aggregates and attenuates the toxicity of mutant huntingtin and α-synuclein [25,28]. However, these chemical chaperones or compounds had little effect on the clearance of mutant Notch3, suggesting that the aggregate formation of mutant Notch3 is not reduced by altering the conditions of the ER or inducing autophagy.

Our studies also have shown that the Tet-on inducible cell lines are a useful cellular system for screening the reagents to dissociate the preformed aggregates of mutant Notch3. One of the advantages of this cellular system is that the effects of compounds can be tested under physiological conditions. It has been considered that low-molecular compounds being active in the cell-free system are often inactivate in vivo, because they are not taken up into cells, they interact nonspecifically with other proteins, or they are metabolized into inactive forms. In addition, the efficacy of many compounds is simply determined by quantitative Western blot analysis. Therefore, this cellular system represents an additional tool for studying the processes occurring during the formation of mutant Notch3 aggregates and therapeutic reagents affecting such processes.

In conclusion, using the Tet-on inducible stable cell lines, we screened for low-molecular compounds that efficiently degrade the preformed aggregates of mutant Notch3. By this method, we found that the degradation of preformed mutant aggregates was enhanced by treatment with either DAPH or SA, which inhibits Aβ fibrillization. Our study may be useful for the development of a pharmacological therapy for CADASIL.

Acknowledgments

We thank Ms. Aki Nagasaki and Ms. Mikiko Matsuzaki for excellent technical assistance. This study was supported by the Program for Promotion of Fundamental Studies in Health Science of the National Institute of Biomedical Innovation (NIBIO), a Research Grant for Longevity Sciences (18C-4) from the Ministry of Health, Labour and Welfare, and Grant-in-Aid for Scientific Research [KAKENHI](21790639 and 22500327).

References

[1] E. Tournier-Lasserve, A. Joutel, J. Melki, J. Weissenbach, G.M. Lathrop, H. Chabriat, J.L. Mas, E.A. Cabanis, M. Baudrimont, J. Maciazek, M.A. Bach, M.G. Bousser, Cerebral autosomal dominant arteriopathy with subcortical infarcts and leukoencephalopathy maps to chromosome 19q12, Nat. Genet. 3 (1993) 256–259.
[2] H. Chabriat, K. Vahedi, M.T. Iba-Zizen, A. Joutel, A. Nibbio, T.G. Nagy, M.O. Krebs, J. Julien, B. Dubois, X. Ducrocq, M. Levasseur, P. Homeyer, J.L. Mas, O. Lyon-Caen, E. Tournier-Lasserve, M.G. Bousser, Clinical spectrum of CADASIL: a study of 7 families. Cerebral autosomal dominant arteriopathy with subcortical infarcts and leukoencephalopathy, Lancet 346 (1995) 934–939.
[3] M.M. Ruchoux, C.A. Maurage, CADASIL: cerebral autosomal dominant arteriopathy with subcortical infarcts and leukoencephalopathy, J. Neuropathol. Exp. Neurol. 56 (1997) 947–964.
[4] M.M. Ruchoux, H. Chabriat, M.G. Bousser, M. Baudrimont, E. Tournier-Lasserve, Presence of ultrastructural arterial lesions in muscle and skin vessels of patients with CADASIL, Stroke 25 (1994) 2291–2292.
[5] J.M. Schröder, B. Sellhaus, J. Jörg, Identification of the characteristic vascular changes in a sural nerve biopsy of a case with cerebral autosomal dominant arteriopathy with subcortical infarcts and leukoencephalopathy (CADASIL), Acta Neuropathol. 89 (1995) 116–121.
[6] A. Joutel, C. Corpechot, A. Ducros, K. Vahedi, H. Chabriat, P. Mouton, S. Alamowitch, V. Domenga, M. Cécillion, E. Maréchal, J. Maciazek, C. Vayssiére, C. Cruaud, E.A. Cabanis, M.M. Ruchoux, J. Weissenbach, J.F. Bach, M.G. Bousser, E. Tournier-Lasserve, Notch3 mutations in CADASIL, a hereditary adult-onset condition causing stroke and dementia, Nature 383 (1996) 707–710.

[7] A. Joutel, K. Vahedi, C. Corpechot, A. Troesch, H. Chabriat, C. Vayssiére, C. Cruaud, J. Maciazek, J. Weissenbach, M.G. Bousser, J.F. Bach, E. Tournier-Lasserve, Strong clustering and stereotyped nature of Notch3 mutations in CADASIL patients, Lancet 350 (1997) 1511–1515.
[8] A. Ishiko, A. Shimizu, E. Nagata, K. Takahashi, T. Tabira, N. Suzuki, Notch3 ectodomain is a major component of granular osmiophilic material (GOM) in CADASIL, Acta Neuropathol. 112 (2006) 333–339.
[9] A. Joutel, F. Andreux, S. Gaulis, V. Domenga, M. Cécillion, N. Battail, N. Piga, F. Chapon, C. Godfrain, E. Tournier-Lasserve, The ectodomain of the Notch3 receptor accumulates within the cerebrovasculature of CADASIL patients, J. Clin. Invest. 105 (2000) 597–605.
[10] H. Karlström, P. Beatus, K. Dannaeus, G. Chapman, U. Lendahl, J. Lundkvist, A CADASIL-mutated Notch3 receptor exhibits impaired intracellular trafficking and maturation but normal ligand-induced signaling, Proc. Natl. Acad. Sci. USA 99 (2002) 17119–17124.
[11] M.M. Ruchoux, V. Domenga, P. Brulin, J. Maciazek, S. Limol, E. Tournier-Lasserve, A. Joutel, Transgenic mice expressing mutant Notch3 develop vascular alterations characteristic of cerebral autosomal dominant arteriopathy with subcortical infarcts and leukoencephalopathy, Am. J. Pathol. 162 (2003) 329–342.
[12] N. Peters, C. Opherk, S. Zacherle, A. Capell, P. Gempel, M. Dichgans, CADASIL-associated Notch3 mutations have differential effects both on ligand binding and ligand-induced Notch3 receptor signaling through RBP-Jk, Exp. Cell Res. 299 (2004) 454–464.
[13] A. Joutel, M. Monet, V. Domenga, F. Riant, E. Tournier-Lasserve, Pathogenic mutations associated with cerebral autosomal dominant arteriopathy with subcortical infarcts and leukoencephalopathy differently affect Jagged1 binding and Notch3 activity via the RBP/Jk signaling pathway, Am. J. Hum. Genet. 74 (2004) 338–347.
[14] W.C. Low, Y. Santa, K. Takahashi, T. Tabira, R.N. Kalaria, CADASIL-causing mutations do not alter Notch3 receptor processing and activation, Neuroreport 17 (2006) 945–949.
[15] S. Ihalainen, R. Soliymani, E. Iivanainen, K. Mykkänen, A. Sainio, M. Pöyhönen, K. Elenius, H. Järveläinen, M. Viitanen, H. Kalimo, M. Baumann, Proteome analysis of cultivated vascular smooth muscle cells from a CADASIL patient, Mol. Med. 13 (2007) 305–314.
[16] C. Opherk, M. Duering, N. Peters, A. Karpinska, S. Rosner, E. Schneider, B. Bader, A. Giese, M. Dichgans, CADASIL mutations enhance spontaneous multimerization of *NOTCH3*, Hum. Mol. Genet. 18 (2009) 2761–2767.
[17] K. Takahashi, K. Adachi, K. Yoshizaki, S. Kunimoto, R.N. Kalaria, A. Watanabe, Mutations in *NOTCH3* cause the formation and retention of aggregates in the endoplasmic reticulum, leading to impaired cell proliferation, Hum. Mol. Genet. 19 (2010) 79–89.
[18] B.J. Blanchard, A. Chen, L.M. Rozeboom, K.A. Stafford, P. Weigele, V.M. Ingram, Efficient reversal of Alzheimer's disease fibril formation and elimination of neurotoxicity by a small molecule, Proc. Natl. Acad. Sci. USA 101 (2004) 14326–14332.
[19] H. Wang, M.L. Duennwald, B.E. Roberts, L.M. Rozeboom, Y.L. Zhang, A.D. Steele, R. Krishnan, L.J. Su, D. Griffin, S. Mukhopadhyay, E.J. Hennessy, P. Weigele, B.J. Blanchard, J. King, A.A. Deniz, S.L. Buchwald, V.M. Ingram, Direct and selective elimination of specific prions and amyloids by 4,5-dianilinophthalimide and analogs, Proc. Natl. Acad. Sci. USA 105 (2008) 7159–7164.
[20] G.T. Westermark, K.H. Johnson, P. Westermark, Staining methods for identification of amyloid in tissue, Methods Enzymol. 309 (1999) 3–25.
[21] W.E. Klunk, H. Engler, A. Nordberg, Y. Wang, G. Blomqvist, D.P. Holt, M. Bergström, I. Savitcheva, G.F. Huang, S. Estrada, B. Ausén, M.L. Debnath, J. Barletta, J.C. Price, J. Sandell, B.J. Lopresti, A. Wall, P. Koivisto, G. Antoni, C.A. Mathis, B. Långström, Imaging brain amyloid in Alzheimer's disease with Pittsburgh Compound-B, Ann. Neurol. 55 (2004) 306–319.
[22] G. Bonapace, A. Waheed, G.N. Shah, W.S. Sly, Chemical chaperones protect from effects of apoptosis-inducing mutation in carbonic anhydrase IV identified in retinitis pigmentosa 17, Proc. Natl. Acad. Sci. USA 101 (2004) 12300–12305.
[23] K. Kubota, Y. Niinuma, M. Kaneko, Y. Okuma, M. Sugai, T. Omura, M. Uesugi, T. Uehara, T. Hosoi, Y. Nomura, Suppresive effects of 4-phenylbutyrate on the aggregation of Pael receptors and endoplasmic reticulum stress, J. Neurochem. 97 (2006) 1259–1268.
[24] U. Özcan, E. Yilmaz, L. Özcan, M. Furuhashi, E. Vaillancourt, R.O. Smith, C.Z. Görgün, G.S. Hotamisligil, Chemical chaperones reduce ER stress and restore glucose homeostasis in a mouse model of type 2 diabetes, Science 313 (2006) 1137–1140.
[25] S. Sarkar, J.E. Davies, Z. Huang, A. Tunnacliffe, D.C. Rubinsztein, Trehalose, a novel mTOR-independent autophagy enhancer, accelerates the clearance of mutant huntingtin and α-synuclein, J. Biol. Chem. 282 (2007) 5641–5652.
[26] F. Yang, G.P. Lim, A.N. Begum, O.J. Ubeda, M.R. Simmons, S.S. Ambegaokar, P. Chen, R. Kayed, C.G. Glabe, S.A. Frautschy, G.M. Cole, Curcumin inhibits formation of amyloid β oligomers and fibrils, binds plaques, and reduces amyloid in vivo, J. Biol. Chem. 280 (2005) 5892–5901.
[27] S.F. de Almeida, G. Picarote, J.V. Fleming, M. Carmo-Fonseca, J.E. Azevedo, M. de Sousa, Chemical chaperones reduce endoplasmic reticulum stress and prevent mutant HFE aggregate formation, J. Biol. Chem. 282 (2007) 27905–27912.
[28] M. Tanaka, Y. Machida, S. Niu, T. Ikeda, N.R. Jana, H. Doi, M. Kurosawa, M. Nekooki, N. Nukina, Trehalose alleviates polyglutamine-mediated pathology in a mouse model of Huntington disease, Nat. Med. 10 (2004) 148–154.

BRAIN and NERVE 62(7)：769-775，2010

特 集 ■ アルツハイマー病 ── 研究と診療の進歩

アルツハイマー病のバイオマーカー

Biological Marker for Alzheimer Disease

松 原 悦 朗*

Etsuro Matsubara*

Abstract

The possibility of that Alzheimer disease (AD)-modifying treatments such as amyloid β-protein (Aβ) immunotherapies being available raises an urgent need for biological markers that will facilitate early and accurate diagnosis. This concept is now widely accepted, because without doubts that such treatments should be initiated during the early stages of the disease. In this review, we discusses the recent progress in identification of biological markers by placing a particular focus on Aβ and tau.

Key words：Alzheimer disease, CSF, Aβ, tau

はじめに

超高齢化社会の到来が確実視されているわが国において，認知症患者は飛躍的に増加し，現在は200万人を突破している。認知症患者の多くを占めるアルツハイマー病（Alzheimer disease：AD）の病態解明と，その治療および診断方法の確立は早急に解決すべき重要な課題である。現在，抗コリンエステラーゼ阻害薬であるドネペジル（アリセプト®）が唯一のAD治療薬として利用されているが，早期からの使用で一過性の効果発現に活路を見出さざるを得ない現状は，認知症診療に関わる臨床医や研究者にとって大きなジレンマである。

われわれは1990年代から，ADの病理学的変化を反映するサロゲートマーカーとして，α1－アンチキモトリプシン（antichymotripsin：ACT），Aβ蛋白（Aβ），タウの脳脊髄液（cerebrospinal fluid：CSF）検査が有用であることを報告してきた[1-4]。しかしながら，根治的な治療法がないという状況において，早期診断を念頭に置いたバイオマーカー開発は，遺伝子診断に匹敵するほどハードルの高いものと捉えられていた。したがって，積極的にこの開発に携わる臨床家・研究者はごくわずかで，われわれがこの時点でその重要性の認識を周囲に求めるのは酷な状況にあった。

こうしたフラストレーションに苛まれる長年の懸案を一掃し，バイオマーカー開発に光明を当てる契機となった特筆すべき報告がAβワクチン開発である。このAβワクチンによる根本的治療法がいよいよADでも利用可能になりそうだとの期待は，これまでハードルの高かった根本治療のための早期診断，その際に不可欠なツールとしてのバイオマーカーに明確な整合性を与え，治療と一体化したADのバイオマーカーとしてその存在意義が認識されるに至った。この結果，バイオマーカー開発には消極的であった多くの研究者も，この領域に参入し現在に至っているわけである。

最近公表されたヒトAβワクチン臨床治験結果では，沈着した老人斑アミロイド除去には成功しているにもかかわらず，神経原線維変化による神経変性と認知症の進行を阻止することができなかったと報告されている[5]。すなわち，アミロイドカスケード仮説（Fig. 1）で，老人斑アミロイドの下流に位置していると考えられる異常リン酸化タウ蓄積やシナプス・神経細胞障害が加速度的に進行している認知症進行例では，老人斑アミロイドを標的とした治療では不十分なこと，したがって認知症の前段階である軽度認知障害（mild cognitive impairment：MCI），さらに認知機能発症前の段階で，こうしたAβワ

* 弘前大学大学院医学研究科脳神経内科学講座〔〒036-8216　青森県弘前市在府町5番地〕Department of Neurology, Hirosaki University Graduate School of Medicine, 5 Zaifu, Hirosaki, Aomori 036-8216, Japan

1881-6096/10/¥500/論文/JCOPY

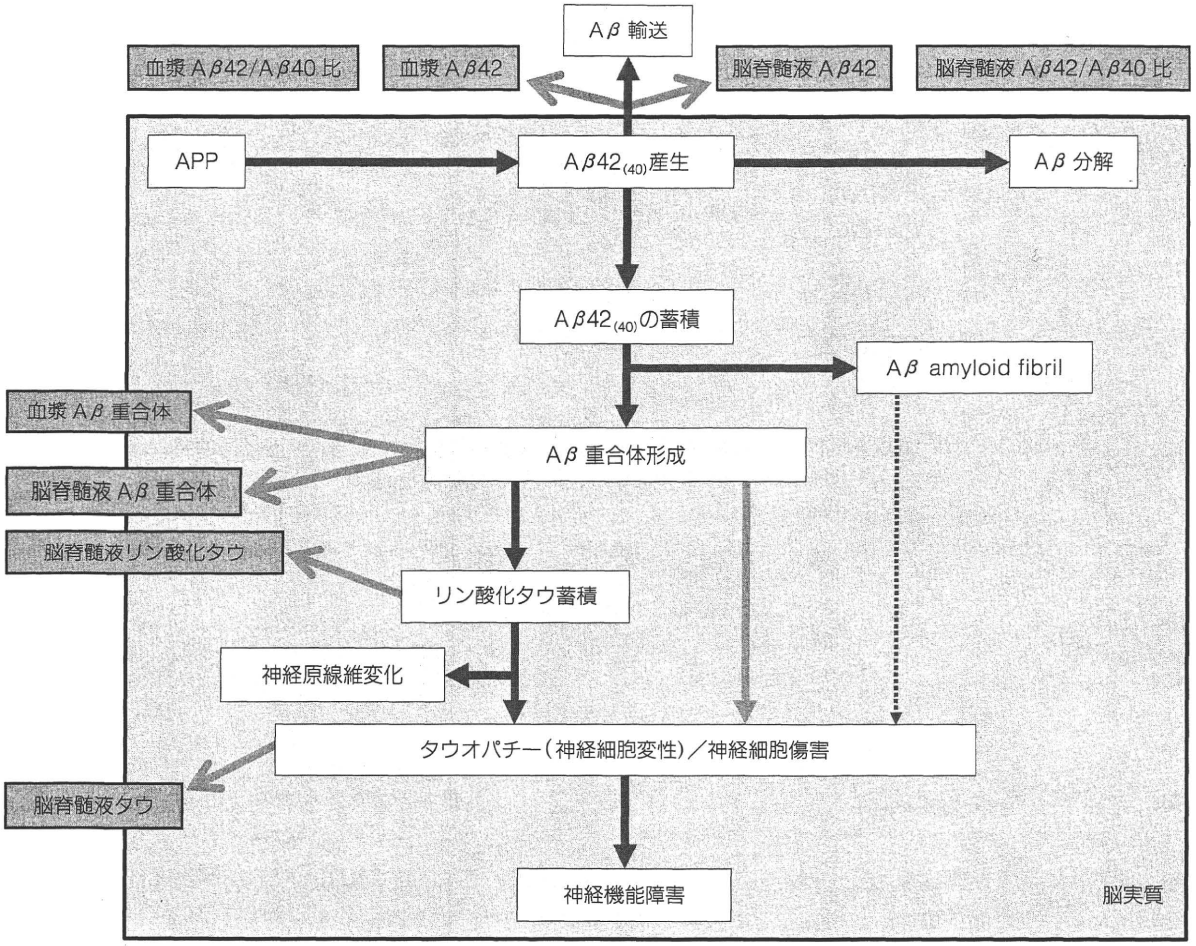

Fig. 1　アミロイドカスケード仮説とバイオマーカーの位置づけ

クチン治療を開始するべきであると考えられるに至った。MCI から AD へと進行し得る患者予測など，バイオマーカーにも発症予測を念頭に置いたスクリーニングバイオマーカーや，特異的に AD 診断を可能とする診断目的のバイオマーカーなど，その開発には予防と治療介入を視野に入れた質的に異なるバイオマーカー開発研究がなされるようになってきている。

Ⅰ．AD におけるバイオマーカー開発の変遷

そもそも，なぜバイオマーカー開発が必要とされたのか？　その発想の原点は，臨床医にとってはおそらく診療精度を高めるツールとして，研究者にとっては飽くなき探求心の賜物としてであったかもしれない。従来 AD の臨床診断は diagnostic and statistical manual of mental disorders, fourth edition (DSM-IV-TR) や national institute of neurological disorders and stroke-Alzheimer disease and related disorders association (NINCDS-ADRDA) といった基準によりなされており，その診断の基本骨子は緩徐進行性の認知症であることと，ほかの疾患や病態が除外されることである。こうした臨床診断基準の問題は，診断特異性は極めて高いものの，診断感度が低く，早期診断，すなわち臨床的な診断に迷う症例で，実際にバイオマーカーが必要となるのにその現実的な活用に難があったことである。臨床診療の有力なツールとしてバイオマーカーを定義するならば，AD のみをほかの認知症疾患から 100%明確に差別化でき，かつその脳病態の現状を如実に反映する分子を，非侵襲的であり，簡便かつ容易な方法で，再現性よく定量的に判定できることである。これまでの研究から AD の病因ならびに発症機構に関して多くの知見が蓄積されてきているが(Fig. 1)，先に述べた知見を基盤として，AD のバイオマーカー開発では AD 患者脳の 2 大病理所見(老人斑と神経原線維変化)の主要構成蛋白検出による脳内病態の推測がまず試みられた。最近は，より直接的でリアルタイムな脳内老人斑蓄積状態の画像化が現実のも

のとなっているが，すべての施設で実施可能な検査にはほど遠い。本稿では，老人斑構成成分としてのAβ，神経原線維変化の構成成分としてのタウの，バイオマーカーとしての知見をアミロイドカスケード仮説に基づき整理し，レビューする。

Ⅱ．脳脊髄液Aβの臨床的検討

従来，AD患者脳に沈着するAβは不溶性で，生成されるとすぐに自己凝集を起こしてアミロイドを形成すると考えられてきた。しかし，1992年の可溶性Aβの発見[6]により，最初は水溶性であるAβがなんらかの機序でβシート構造に富む二次構造変化を獲得し，アミロイド線維が形成されることが明らかとなった。こうした可溶性Aβが脳脊髄液中に存在するという報告[6]が契機となり，脳脊髄液Aβのバイオマーカーとしての検証が開始された。そのバイオマーカーとしての飛躍的進歩は，Suzukiら[7]によるAβ40/42を分別定量する高感度ELISA（enzyme-linked immunosorbent assay）法の開発によりもたらされたが，これは日本が世界に誇るべき業績の1つである。特に，同ELISAでも使用されているAβ40/42断端特異的抗体により，Aβ42がAD脳内に早期から蓄積し[8]，ADの発症惹起分子であるとも明らかとされたことは，脳脊髄液Aβのバイオマーカー検証に多大な貢献となった。Aβは主に神経細胞で産生され，生理的な条件下では脳内分解や脳外輸送により脳内での蓄積を免れているが，AD患者脳ではそれらいずれかの機能低下の結果Aβの脳内蓄積をきたしていると考えられている（Fig. 1）。1995年，こうしたAβクリアランスの低下を反映し，特にAβ42の選択的低下がAD患者の脳脊髄液中で実際に認められることが最初に報告された[9]。この報告は小規模研究ながら，現在最も信頼のおける脳脊髄液Aβ42の選択的低下の先駆的な報告であった。1998年にわれわれは日本発の多施設大規模追跡研究（GTT1：Gunma Tottori Tohoku）を施行し[10]，世界に先駆けAβ40/42 ratioのバイオマーカーとしての診断感度・特異度がそれぞれ56%，73%と報告した。2002年にはこの倍以上の規模でGTT1が再検討され（GTT2）[11]，診断感度はそれぞれ59%，88%と報告された。2003年にこれまでの報告のメタ解析の結果が『JAMA』誌[12]に公開され，脳脊髄液Aβの臨床的エビデンスが確認されたが，結果的にはより大規模での前向き研究によるエビデンス確立が必要と結論づけられた。こうした背景を反映して，MCI症例からADへの進行予測を中心とした前向き検討が本格化し，総じて脳脊髄液Aβ42の低下の重要性が確認されている。55例のMCIを追跡したParnettiらの研究[13]では，ADを発症した10/11例（progressive MCI）で，既にMCIの段階から脳脊髄液Aβ42が低下していたこと，一方ADへと進行しないMCI（stable MCI）では，脳脊髄液Aβ42に変化を認めなかったと報告している。また，10カ月間52例のMCIを追跡した前向き研究[14]では脳脊髄液Aβ42の低下のAD発症予測感度は59%，特異性は100%であったと報告されている。

Ⅲ．脳脊髄液タウの臨床的検討

タウ蛋白は神経細胞の軸索輸送を担う45～55 kDaの微小管付随蛋白質で，チュブリンが重合して微少管を構成する際の促進因子として機能している。このタウ蛋白は，AD脳では高度なリン酸化を受け凝集・不溶化して神経細胞内に神経原線維変化として蓄積している。ADと異なり，このタウのみが蓄積して神経細胞変性・神経細胞死を起こす疾患はタウオパチーと呼ばれ，前頭側頭型認知症（frontotemporal dementia：FTD），進行性核上麻痺，大脳皮質基底核変性症，嗜銀顆粒病，神経原線維変化型認知症，など非AD型認知症が知られている。

ヒト脳においては選択的スプライシングにより6つのアイソホームが発現しているが，脳脊髄液中ではその多くは微小管結合領域近くで切断され，25～32 kDaの一部がリン酸化されたN末端側断片として存在している。現在，脳脊髄液タウのELISA測定系にはこうしたリン酸化の有無にかかわらず，すべてのアイソホームを検出する総タウ測定系と，特定のリン酸化部位を認識する抗体を用いたリン酸化タウ測定系が開発され，測定キットが市販されている。

脳脊髄液総タウは加齢により軽度の増加を示し[15]，神経細胞自体の破壊・損傷の起こる先のタウオパチーや急性期脳梗塞・脳挫傷，また軸索変性を合併するギラン・バレー症候群[16]や多発性硬化症[17]でも脳脊髄液総タウの上昇を認める。こうした欠点を補う目的で，AD脳に蓄積する高度にリン酸化されたタウのみを選択的に検出するELISA［Thr181部位特異的（Innogenetics社），Ser199部位特異的（三菱化学社），Thr231部位特異的（Innogenetics社），Ser235部位特異的（Applied NeuroSolution社）リン酸化タウを検出］が開発され，前述した疾患でも正常化わずかな上昇を認めるのみで[17-19]，AD脳内の病態（神経細胞内リン酸化タウ蓄積）を特異的に反映していると考えられている。

脳脊髄液タウのバイオマーカーとしての検証報告も脳

脊髄液Aβ42同様，1995年になされた。少数例の検証ではあったが，わが国においてもAraiらによりその診断感度・特異性が100%と報告された。1998年，われわれが施行したGTT1[10]では，総タウはAD脳脊髄液中で有意に上昇していたものの，診断感度40%，特異性86%であった。2002年に施行した1,000例を超す多施設共同研究（GTTO：Gunma Tottori Tohoku Osaka）では，脳脊髄液総タウによるADの診断感度は59.1%であった。一方，正常コントロールのみとの特異性は96.7%と良好であったが，非認知症神経疾患を含めた特異性は89.5%とオーバーラップの課題が残った。翌2003年に，脳脊髄液総タウについてこれまで報告された世界21施設，2,366例のAD群，1,255例の正常対照群でのメタ解析の結果が『JAMA』誌[12]に公開され，平均感度82%，平均特異性89%と臨床的エビデンスが確認された。しかしながら，神経細胞自体の破壊・損傷の結果，脳脊髄液総タウは上昇するため，AD以外の他疾患とのオーバーラップが問題となった。こうした課題を克服し，より診断精度向上を目指すため，AD脳に特徴的な高度にリン酸化された蓄積タウが測定された。

同一検体を用いた3種類のリン酸化タウ測定キット（Thr181，Ser199，Thr231）の比較検討を検証すると，興味深いことに，Thr181リン酸化タウ測定はADとDLB（dementia with Lewy body）の鑑別に優れ（診断感度94%，特異性64%），Thr231リン酸化タウ測定はADとFTD鑑別（診断感度88%，特異性92%）に優れることが2004年Hampelら[20]により報告された。また，Araiら[21]は，ADのPHF（paired helical filaments）で検出されるSer262のリン酸化部位はピック球やグリア内タウ封入体（進行性核上麻痺・皮質基底核変性症）では検出されにくいと報告しており，Ser262リン酸化タウの測定は，Thr181リン酸化タウ測定でのDLB鑑別，Thr231リン酸化タウ測定でのFTD鑑別など，AD診断においてより疾患特異性の高い脳脊髄液リン酸化タウ測定開発のため，各種タウオパチーにおけるタウのリン酸化部位の相違利用を考慮すべきと考えられる。

2000年以降，Aβと同様に早期ADからMCIへと研究対象がシフトし，早期診断よりも発症予測的利用の是非の検証が多くなった。Araiら[22]は縦断研究でADへと進行したprogressive MCIは，stable MCIよりも脳脊髄液リン酸化タウ値が高いことを報告した。また，Herukkaらの3.5年にわたる追跡調査[23]でも，脳脊髄液リン酸化タウ値の上昇と，さらに総タウも有意に高値であることが報告された。

Hanssonら[24]とLewczukら[25]の多施設長期追跡調査では，認知症に移行するMCIでは脳脊髄液総タウ値が高いが，ADに移行するMCIでは脳脊髄液総タウに加え，Thr181リン酸化タウ値も高いことが報告された。Buergerら[26]は77例のMCIを検討し，ADに進行したMCIの82%でThr231リン酸化タウ値が有意に高く，1年間のMMSE（mini-mental state examination）の低下値とは逆相関が認められた。その後，同グループはThr181，Ser199でも同様の報告をしている[27]。Hampelら[28]は52例のMCIを検証し，ADに進行したMCIの脳脊髄液総タウの測定で診断感度83%，特異度90%と報告した。以上の結果より，MCIからADへの進行予測に脳脊髄液リン酸化タウ測定は有用であると考えられる。

Ⅳ．脳脊髄液Aβと総タウまたはリン酸化タウの組み合わせ

これまで述べてきたAβとタウの組み合わせで，ADの診断感度，特異性を向上させることが可能である。われわれが施行したGTT1[10]では，AD index（＝[Aβ40/42]×総タウ）を設定するとAβ40/42，総タウ単独では56%/73%，40%/86%であった感度／特異性を，それぞれ71%/81%まで向上させることができた。これまで世界的に施行された多施設大規模追跡研究，コミュニティー前向き研究，システムレビュー，剖検病理所見との対応，メタ解析の報告を総合すると，脳脊髄液Aβ42の低下と総タウ増加の組み合わせで，診断感度71～94%，診断特異性80～100%と臨床使用に満足すべきエビデンスの報告がなされている。

さらに，MCIからADへの発症予測に関する前向き研究でも，脳脊髄液Aβ42の低下と総タウ増加の組み合わせで，予測感度（89～95%）や特異性（83～87%）に満足すべき結果が得られている。特にFaganら[29]により報告された総タウ／Aβ42もしくはリン酸化タウ／Aβ42が増加している症例では，健常者からADへの発症予測が可能であるとの報告は注目に値する。最近になり，われわれも参加しているJ-ADNIの米国版US-ADNI研究結果の一部が，昨年『Ann Neurol』誌に報告された[30]。100例の早期AD，196例のMCI，114例の高齢健常者でのバイオマーカー検索と病理検索（AD脳56例，高齢健常者脳52例）がなされ，病理検索対照群では総タウ／Aβ42比の予測感度は85.7%，特異性は84.6%と高く，1年以内にADを発症した37例のMCIのうち33例（89%）をAD発症前に診断可能であったと報告されている。最近平均2年程度の前向き研究[31]で，脳脊髄液Aβ42/[240＋(1.18×総タウ)]の上昇を呈するMCI症